+ MODEL

Available online at www.sciencedirect.com

ScienceDirect

Solid Earth Sciences 9 (2024) 100199

www.elsevier.com/locate/SESCI

The slab failure in Central Java (Indonesia): New insight into its tectonic setting and origin

Shaban Godang [a], Sugeng Purwo Saputro [b], Huan Li [c,*]

[a] Independent Geochemist, Geochemistry Tectonic Modeling, and REE Researcher, Jakarta, 11470, Indonesia
[b] Research Center for Geological Resources, National Research and Innovation Agency (BRIN), Bandung, 40135, Indonesia
[c] School of Geosciences and Info-Physics, Central South University, Changsha, 410083, China

Received 21 June 2024; revised 9 August 2024; accepted 11 August 2024
Available online ■ ■ ■

Abstract

The geochemical and tectonic characteristics of volcanic formations in Central Java, specifically the Sumbing-Slamet volcanics, were investigated to understand the processes associated with slab failure in the region. Through comprehensive geochemical analysis and comparison with other volcanic formations, insights into the magmatic evolution and tectonic settings of the Sumbing-Slamet volcanics were gained. The findings support the hypothesis of slab tearing beneath Central Java, as evidenced by distinct geochemical signatures and magmatic interactions observed in the Sumbing-Slamet volcanics. Geochemical data reveal medium to high potassium content (K_2O = 0.77–2.32%), low Nb/Y (<0.6561), low TiO_2 relative to Al_2O_3 [$TiO_2 < (-1.1610 + 0.1935 \times Al_2O_3)$], Th/La >0.2, as well as a wide range of Nb/La and Nb/Zr (0.14–0.89 and 0.0304–0.0744, respectively), notable depletions in high-field strength elements (HFSE; such as Nb, Ti), low to high Ta-anomaly (δTa = 0.21–1.03), and whole-rock isotopes of $^{87}Sr/^{86}Sr$ (0.704458–0.705800) and $^{143}Nd/^{144}Nd$ (0.513059–0.512766) demonstrate that they were formed from active continental margin (ACM) tectonics involving subducted sediment input. These magmatic processes likely resulted from the mixing of lithospheric and asthenospheric mantle sources due to slab failure in the northern part of Central Java. The research contributes to strengthening the geophysical view regarding the existence of slab tearing in Central Java, understanding the dynamic geological processes occurring in subduction zones, and emphasizing the importance of interdisciplinary approaches in studying such phenomena.

Keywords: Slab failure; Central Java; Sumbing and Slamet volcanics; Active continental margins (ACM); Tantalum anomaly (δTa); Lithospheric and asthenospheric mantle sources

1. Introduction

The geotectonic formation of Java Island, which is part of the Sunda arc of Indonesia, has been studied for many years, yielding numerous varied interpretations (Sugimura, 1968; Hamilton, 1979; Lee et al., 2012; Gardner et al., 2013; Harijoko et al., 2016; Mulyaningsih and Shaban, 2020). Central Java, with its distinctive geometric shape (narrowing; see Fig. 1), has become the most intriguing area for investigation by geophysicists, owing to the possibility of large-scale geological structures controlling the region (Katili, 1978; Widiyantoro et al., 2011; Handley et al., 2014). Seismic tomography studies have revealed the presence of oceanic slab tearing beneath the subduction zone of Central Java, along with the identification of magma whose constituent material originates from the asthenosphere (Puspito et al., 1993; Widiyantoro and van Der Hilst, 1996, 1997; Widiyantoro et al., 2011). These findings are particularly compelling, especially in relation to the megathrust in southern Java.

Further research employing geochemical approaches has also been conducted to substantiate these findings. The combination of geochemical modeling of major elements, trace elements, and rare earth elements (REEs), which is sensitive to

* Corresponding author.
E-mail address: lihuan@csu.edu.cn (H. Li).
Peer review under responsibility of Guangzhou Institute of Geochemistry.

https://doi.org/10.1016/j.sesci.2024.100199

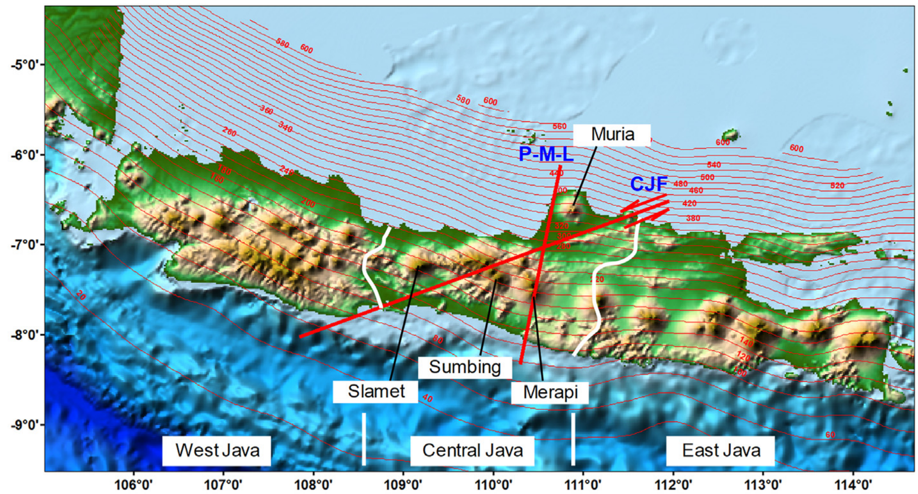

Fig. 1. The Java topographic map, showing the locations of Sumbing, Slamet, Merapi, and rear-arc Muria volcanoes in Central Java. Red lines show the depth of the Benioff zone beneath Java Island (after Hamilton, 1979). The Central Java Fault (CJF; after Chotin et al., 1984; and Hoffmann-Rothe et al., 2001). The inferred Progo-Muria Lineament (P-M-L; adapted from Smyth et al., 2005 and 2007; and Handley et al., 2014).

geochemical discrimination and can be applied to mafic-felsic rocks simultaneously, is expected to yield results and provide a more detailed explanation of this phenomenon. However, the geochemical discrimination generated thus far still falls short of providing a detailed explanation of the phenomenon of slab tearing in Central Java (Hatherton and Dickinson, 1969; Vukadinovic and Sutawidjajat, 1995; Gertisser and Keller, 2003; Fadlin et al., 2021). Much of it remains confined to discrimination regarding island arcs (IA), active continental margins (ACM), melanges, etc (Coleman, 1975; Whitford et al., 1979; Handley et al., 2008; Frisch et al., 2011). The latest geochemical discrimination theory regarding slab break-off (slab failure) in subduction zones was proposed by Whalen and Hildebrand (2019), but its application is still limited to granitic rocks and requires adjustments in certain aspects.

In this study, particular attention is given to the geochemical evolution associated with oceanic slab failure significantly contaminated with mantle originating from different magmatic sources. Here, we focus on the use of whole rock geochemistry on the Sumbing and Slamet volcanics in Central Java, which represent magmatism associated with a significant slab failure effect, while comparing them with other volcanics (Merapi and rear arc Muria volcanics; Agung volcanics, Bali Island; and Candlemass-Vindication volcanics, South Atlantic Ocean). The results of this study significantly enhance our understanding of ACM tectonics, specifically which manifestations of magmatism contain entirely continental components, which ones significantly interact with other magmatic sources due to slab tearing, and which ones are unrelated to subduction (despite their location in the rear arc).

2. Geological background and mineralogy

The island of Java is situated in the central section of the Sunda arc, which extends from the Andaman Islands north of Sumatra to Flores in the Banda Sea. The Sumbing and Slamet volcanoes, located in Central Java, are Tertiary to Quaternary volcanoes formed by subduction between the Eurasian and Indian-Australian plates on the southern side of Indonesia in the Benioff zone (Leterrier et al., 1990; Kundu and Gahalaut, 2011) (see Fig. 1).

The main structural features and geological division can be inferred between Central Java and East Java, running approximately northeast-southwest (NE–SW) through Java Island, close to Merapi at the fore-arc and Muria volcano at the rear of the arc (see Fig. 1). This lineament is described as a strike-slip Central Java Fault (CJF; Chotin et al., 1984; Hoffmann-Rothe et al., 2001) or the inferred Progo-Muria Lineament (P-M-L; Smyth et al., 2005 and 2007; Handley et al., 2014) and is suggested to mark the eastern limit of accreted Cretaceous terranes and sutures (Hoffmann-Rothe et al., 2001) or the western limit of Archean-aged zircons in the southern mountains (Smyth et al., 2007), respectively.

The Sumbing volcanic deposits are generally pyroclastic and lavas with a basaltic to andesitic composition and assemblages of plagioclase, clinopyroxene, and titanomagnetite (Dempsey, 2013), whereas the Slamet volcanic deposits are primarily composed of scoria ash and lavas with a basaltic to andesitic composition and assemblages of phenocryst plagioclase, clino-pyroxene, hornblende, and magnetite plus olivine or orthopyroxene (Vukadinovic and Sutawidjajat, 1995; Harijoko et al., 2020). In general, there are no mineralogical differences between these two volcanoes.

3. Materials and geochemical data

We utilized more recent geochemical data (from 2000 onwards) encompassing major, trace, and REEs, including Tantalum (Ta). The Ta-anomaly ($\delta Ta = dTa$; the dTa is read as delta Ta) serves as an indicator for determining magmatic interactions. dTa is calculated by the following equation:

$$\delta Ta\ (=dTa) = (Ta/Ta_{(PM)})\ /\ ((La/La_{(PM)} \times Ce/Ce_{(PM)})\hat{}(1/2))$$

$$\delta Ta\ (=dTa) = (Ta/0.037)\ /\ ((La/0.648 \times Ce/1.675)\hat{}(1/2))$$

$Ta_{(PM)} = 0.037$; $La_{(PM)} = 0.648$; $Ce_{(PM)} = 1.675$; Primitive Mantle (PM) values from McDonough and Sun (1995).

Data for the Sumbing volcanics were sourced from Dempsey (2013), while data for the Slamet volcanics were obtained from Reubi et al. (2002) and Harijoko et al. (2020, 2021). For comparison, geochemical data from the Merapi volcanics (Gertisser and Keller, 2003) and the Muria volcanics (Kirchenbaur et al., 2022) were utilized, representing the most typical volcanic rocks resulting from ACM tectonics and back-arc volcanoes, respectively. Additionally, data from the Agung volcanics on the island of Bali (Dempsey, 2013) were included, which also represent products of ACM tectonics involving the melting of oceanic slabs. Furthermore, typical IA volcanic data from Candlemass-Vindication in the South Atlantic Ocean (Leat et al., 2003) were incorporated for comparison purposes.

4. Results

4.1. Major and trace elements geochemistry

The 20 samples of Sumbing volcanic rocks exhibit SiO_2 content ranging from 53.08% to 61.70%, low TiO_2 concentrations ranging from 0.59% to 1.01%, high Al_2O_3 levels ranging from 17.09% to 19.71%, moderate K_2O concentrations ranging from 1.51% to 2.32%, and low MgO content ranging from 2.14% to 3.93% (with Mg# ranging from 38.33 to 46.82). Additionally, they demonstrate relatively low La/Yb ratios ranging from 6.02 to 10.23, low to moderate Nb/Y ratios ranging from 0.14 to 0.53, and Nb/La ratios ranging from 0.15 to 0.65 (see Appendix A Tables 1 and 2).

The Slamet volcanic rocks, collected in 61 samples, display SiO_2 content ranging from 48.50% to 59.04%, with TiO_2 concentrations varying from low to high (0.58%–1.72%), high Al_2O_3 content ranging from 15.74% to 18.91%, moderate K_2O concentrations ranging from 0.77% to 2.17%, and low to moderate MgO content ranging from 2.45% to 7.85% (with Mg# ranging from 33.18 to 57.84). Moreover, they exhibit low to moderate La/Yb ratios ranging from 3.91 to 17.78, low to moderate Nb/Y ratios ranging from 0.15 to 0.49, Nb/La ratios ranging from 0.14 to 0.89, and a higher Th/La ratio exceeding 0.2 (see Appendix A, Tables 1 and 2).

The results of the K_2O–SiO_2 and Zr/Ti–Nb/Y relationship plots (Figs. 2 and 3) show the magmatic alkalinity series of the Sumbing-Slamet volcanics consists of a medium-to high-K series and are sub-alkaline in nature (Nb/Y < 0.6561). The magmatism of these medium-to high-K series is interpreted to be related to the partial melting of the normal DMM (depleted MORB mantle) and PM (primitive mantle) (Fig. 4), as shown

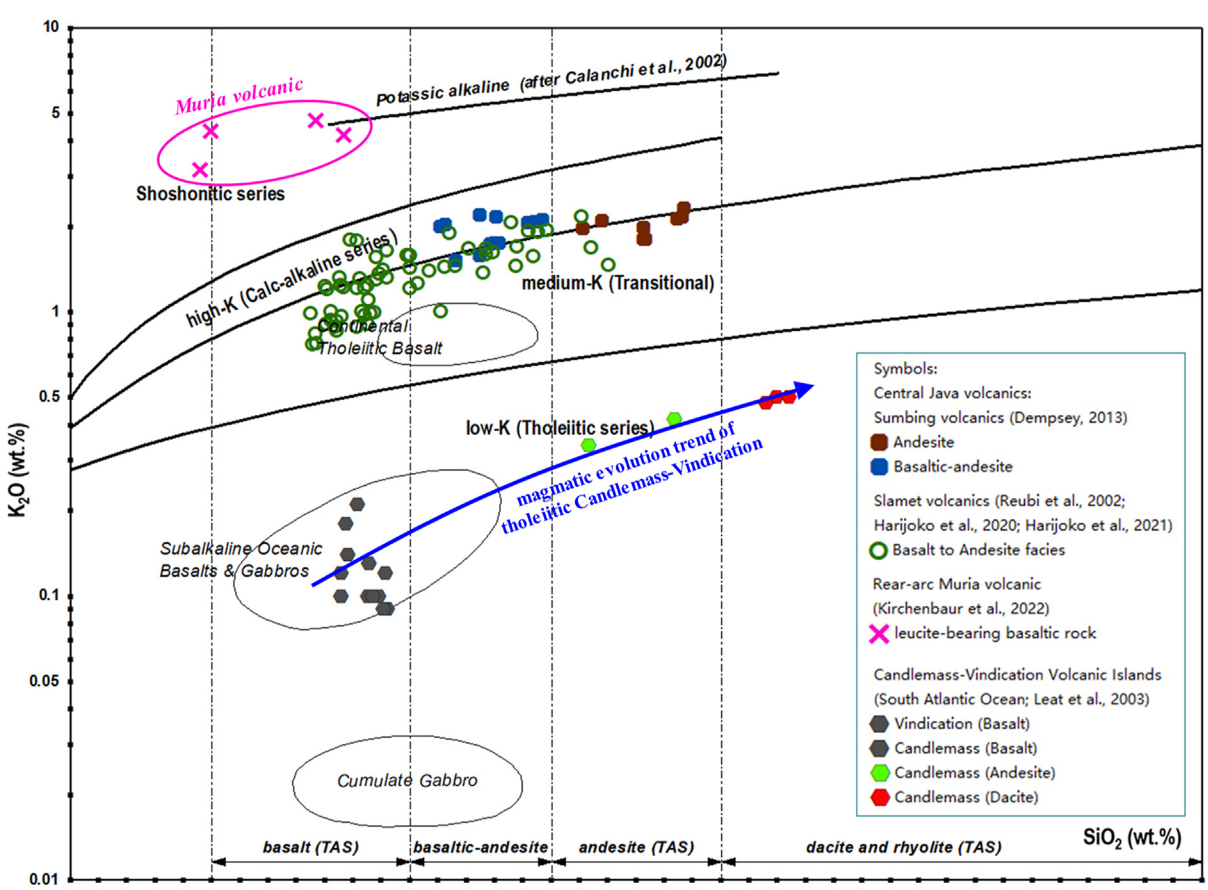

Fig. 2. The overlay diagram of the magmatic alkalinity series (after Peccerillo and Taylor, 1976). The discrimination of cumulate gabbro, subalkaline oceanic basalts and gabbros, and continental tholeiitic basalts (adopted from Coleman and Peterman, 1975). Potassic Alkaline (after Calanchi et al., 2002).

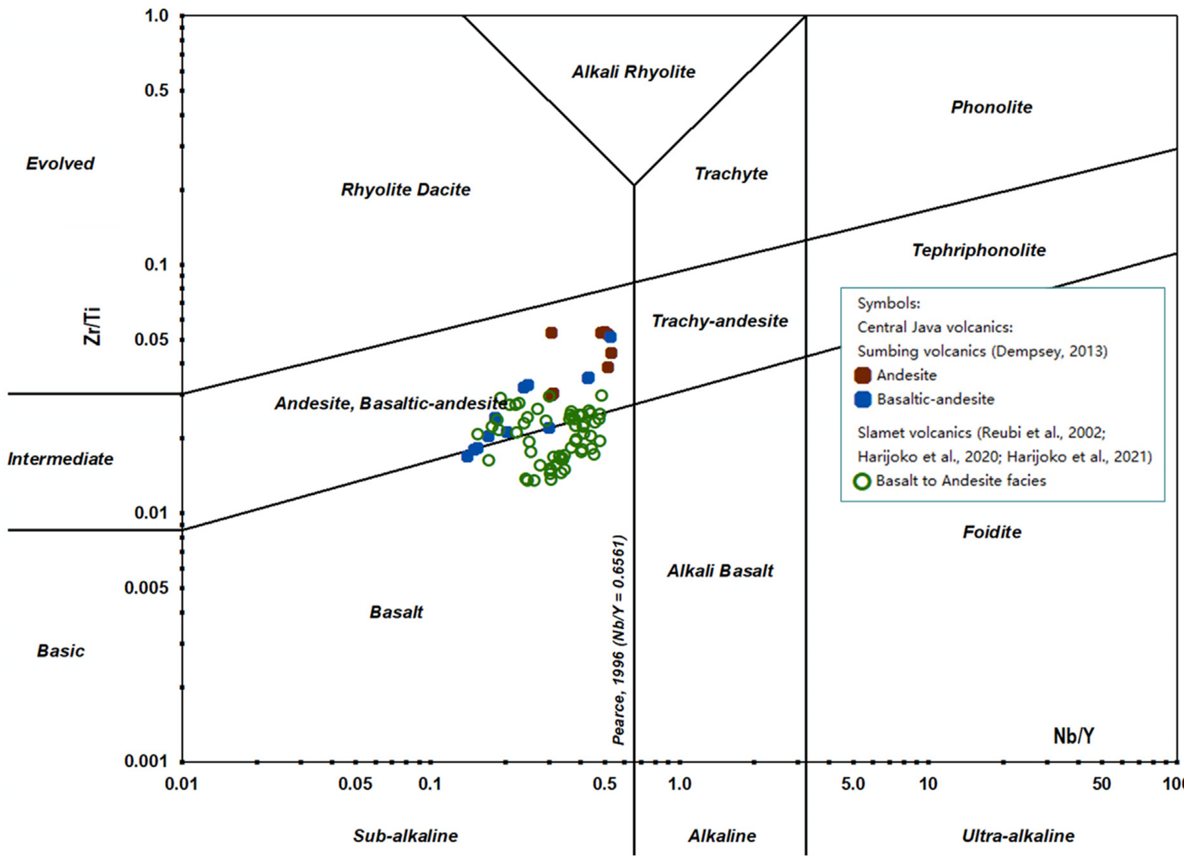

Fig. 3. The volcanic rock classification diagram based on immobile trace elements (Zr/Ti vs. Nb/Y; Pearce, 1996).

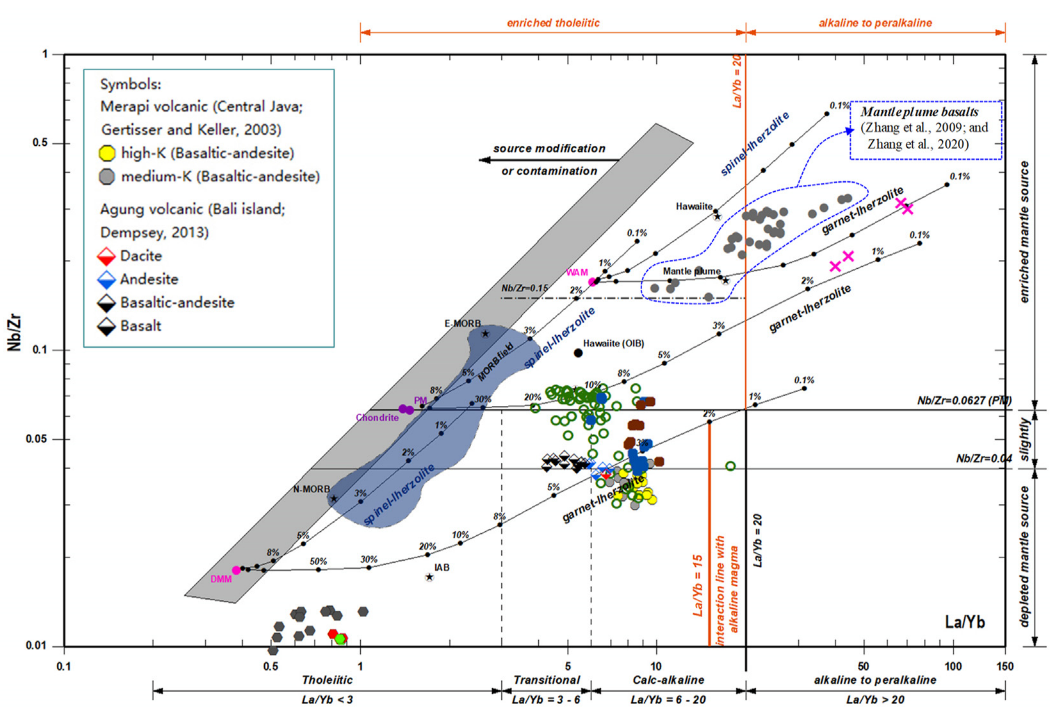

Fig. 4. Partial melting curves of mantle genomes (modified after Aldanmaz et al. (2006) and adapted also from Le Roex et al., 1983; Barrett and MacLean, 1997; Sun et al., 2006; Shaban et al., 2016). The discrimination between an enriched tholeiitic and an alkaline/peralkaline for the enriched mantle source, and the discrimination between calc-alkaline and alkaline/peralkaline for depleted to slightly enriched mantle sources are set by La/Yb = 20 (adopted from Saputro et al., 2022). Other symbols are in Fig. 2. Mantle plumes are from the Wan-Su Basalts (Eastern China; Zhang et al., 2009) and Weizhou Island Basalt (Hainan, China; Zhang et al., 2020).

in the plot results that fall in the lithospheric to mixed lithospheric-asthenospheric mantle sources (Fig. 5). Also, these magma are interpreted to be generated from the ACM tectonics (Fig. 7) and exhibit some magmatic evolution (Figs. 7 and 9). Th/Nb values transitioning from high to low and low to high for Nb/Zr values, as well as breaking through the threshold of Nb/Zr = 0.0627, provide evidence for this magmatic-geochemical evolution.

Furthermore, the spidergram patterns of trace elements in the Sumbing and Slamet volcanics are characterized by distinct negative spikes in Nb and Ti, transitioning from spike to unspike in Ta, with Ta-anomaly (dTa) values ranging from 0.21 to 0.83 and 0.25 to 1.03, respectively (Figs. 10 and 11).

Figs. 10–14 demonstrate that Sumbing-Slamet and Merapi exhibit the same spidergram patterns of trace elements and REEs. Additionally, they show relatively similar Europium anomalies (dEu) and total REE + Y values.

4.2. The Nd–Sr isotopes

Sumbing volcanic deposits exhibit whole-rock isotopic compositions with $^{87}Sr/^{86}Sr$ ratios ranging from 0.704458 to 0.705759 and $^{143}Nd/^{144}Nd$ ratios ranging from 0.513059 to 0.512769. Slamet volcanic deposits display isotopic ratios of $^{87}Sr/^{86}Sr$ ranging from 0.705240 to 0.705800 and $^{143}Nd/^{144}Nd$ ranging from 0.512869 to 0.512766. Meanwhile, Merapi volcanics feature isotopic ratios of $^{87}Sr/^{86}Sr$ ranging from 0.705014 to 0.705826 and $^{143}Nd/^{144}Nd$ ranging from 0.512779 to 0.512675. The back-arc Muria volcanic rocks exhibit isotopic compositions with $^{87}Sr/^{86}Sr$ ratios ranging from 0.704184 to 0.704697 and $^{143}Nd/^{144}Nd$ ratios ranging from 0.512752 to 0.512572 (Appendix A, Table 3). Plotting these data on a $^{143}Nd/^{144}Nd$ vs. $^{87}Sr/^{86}Sr$ diagram (Fig. 15) reveals that the isotopic signatures of the Muria volcanics are not correlated with those of the Sumbing-Slamet-Merapi volcanics.

5. Discussion

5.1. Mantle sources and tectonic settings of Sumbing-Slamet volcanics

The Sumbing and Slamet volcanics exhibit relatively lower TiO_2 compared to Al_2O_3 [$TiO_2 < (-1.1610 + 0.1935 \times Al_2O_3)$] and high Th/La ratios (>0.2) (see Appendix A Tables 1 and 2). These characteristics were interpreted to originate from arc-related magmatism (Müller and Groves, 1993; Shaban et al., 2016), reflect the involvement of continental crustal material (Wang et al., 2016), and also involve subducted sediment input (Schaen et al., 2016). Both volcanics also possess low MgO (ranging from 7.85% to 2.14%), Mg# (ranging from 57.84 to 33.19), and Cr contents (below 260 ppm) (see Appendix A Tables 1 and 2), indicating that the magma did not originate from a primary melt but rather from evolved magma derived from a mixture of garnet-DMM and garnet-PM sources (Aldanmaz et al., 2006; see Fig. 4). Furthermore, Slamet volcanic (one piece of sample) is also interpreted to have interacted with other alkaline magma originating from deeper subduction, as exhibited by La/Yb > 15.

A closer examination in Fig. 5 reveals that the magmatism of Sumbing-Slamet volcanics exhibits low Nb/Y values (<0.6561), characterizing its calc-alkaline nature (Pearce, 1996) and indicating formation within a continental arc at the ACM. This interpretation is consistent with the results from Fig. 7. Further, the Sumbing-Slamet volcanics are also characterized by a wide range of Nb/La (0.15–0.89), some of Nb/Y > 0.4 and Nb/Zr > 0.0627 (Figs. 5, 7 and 9), and dTa values (0.21–1.03; Figs. 10 and 11). A dTa value of 0.8 is equivalent to Nb/La = 0.6, where dTa >0.8 represents magmatic interaction between lithosphere and asthenosphere mantle sources. Both magmatisms are inferred to have originated from the interplay between garnet-DMM and enriched mantle sources of PM (as depicted in Figs. 7 and 9), consistent with the previous interpretation using the Aldanmaz diagram (Fig. 4). This interplay resulted from the mixing of lithospheric and asthenospheric mantle sources (marked by a ratio of Nb/Y > 0.4 and Nb/La >0.6 in Fig. 5) due to slab break-off in Central Java (see the cartoon illustration in Fig. 16), with contamination volumes of asthenospheric mantle source around 50% in Slamet and 40% in Sumbing volcanics (see the magmatic evolution trend in Fig. 7).

We underline that the dNb value (Nb-anomaly) is not taken into account because its position on the normalized diagram depends on the variables to the left and right of Nb, namely U and La (see the latest quantification of the elemental incompatibility sequence from Zhang, 2014, in Figs. 10 and 11). The U value is greatly influenced by the input of subducted sediment (Hawkesworth et al., 1997; Pettke et al., 2018) and rutile eclogite melts (Foley et al., 2002), so its position is often out of balance with respect to La; therefore, it is not appropriate to use it for calculating dNb values. Besides, in using whole-rock geochemistry for determining tectonic settings or those related to magmatic interactions, the dNb value is not as sensitive as dTa (see the geochemical investigation of Southwest Indian Ridge 64°E from Dong et al., 2021; see also the interpretation of the geotectonic and origin of the Anak Krakatau volcanics, Indonesia, by Gardner et al., 2013).

The whole-rock Sumbing-Slamet volcanics have isotopic $^{87}Sr/^{86}Sr$ (0.704458–0.705800) and $^{143}Nd/^{144}Nd$ (0.513059–0.512766), which show that they were formed from subduction continental arc-related magmatism (see the isotopic trend in Fig. 15). Some of the $^{87}Sr/^{86}Sr$ isotopes have relatively low values (0.70480, εSr <0), indicating that they have a contextual relationship with mantle-related processes.

Our new interpretation of the tectonic and genesis of Sumbing-Slamet volcanics, using a combination of geochemical models, isotopic Nd–Sr, and the use of dTa, provides new insights into magmatism in Central Java. Our interpretation complements the geophysical studies utilizing seismic profiles and confirms the presence of slab tearing in Central Java (Koulakov et al., 2007; Cottam et al., 2010; Widiyantoro et al., 2011; Hall and Spakman, 2015) (see Fig. 16) and is also consistent with the previous findings of Kundu and Gahalaut (2011) and Yu et al. (2022), who suggested upwelling of the

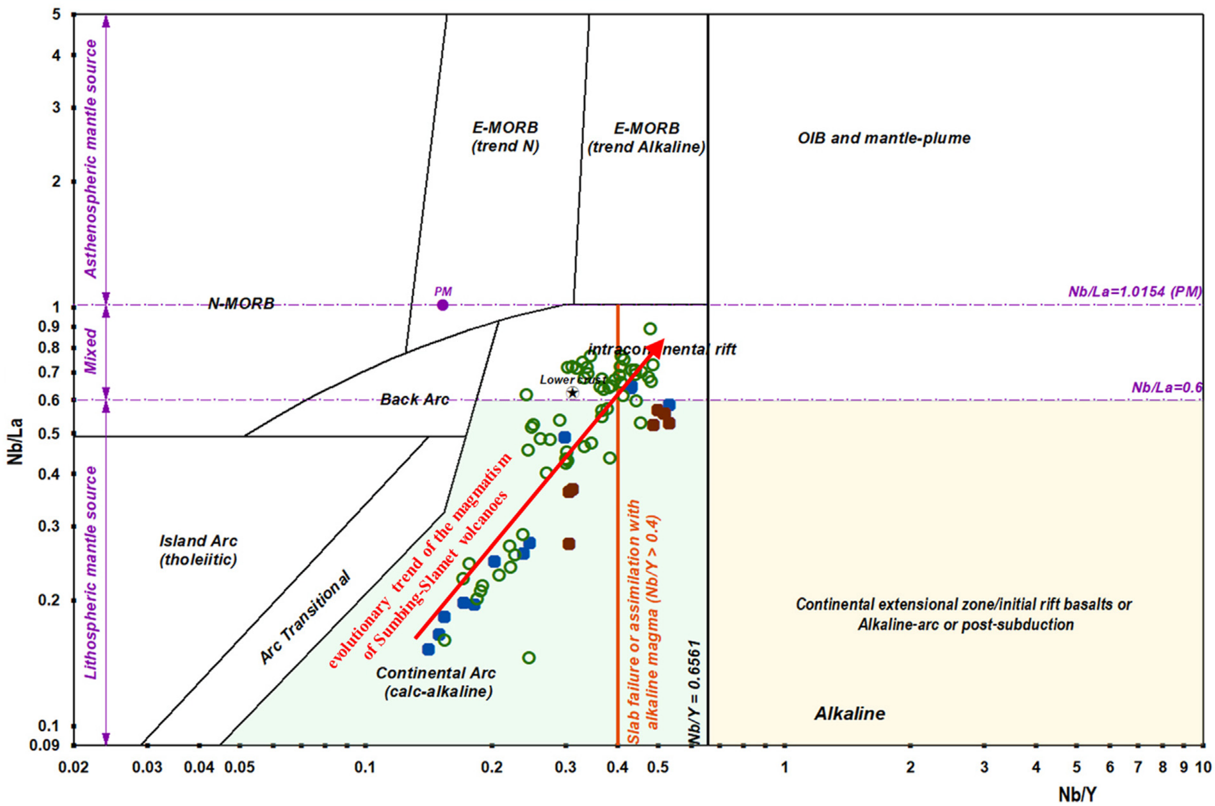

Fig. 5. The tectonic discrimination diagram of Nb/La vs. Nb/Y (constructed from Cabanis and Lecolle, 1989; Pearce, 1996; Abdel-Rahman, 2002; Whalen and Hildebrand, 2019). Symbols for Sumbing and Slamet Volcanics in Fig. 2.

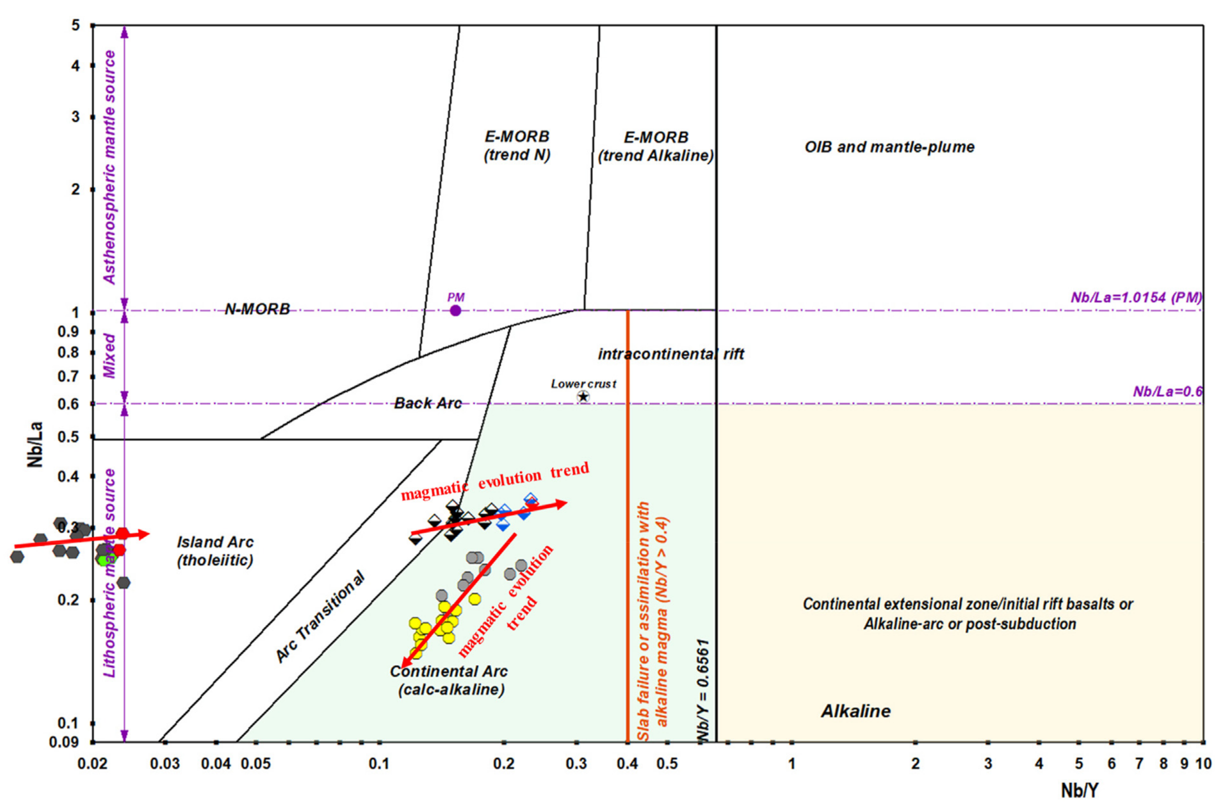

Fig. 6. The tectonic discrimination diagram of Nb/La vs. Nb/Y. Symbols for Merapi, Agung, and Candlemass-Vindication Volcanics in Figs. 2 and 4.

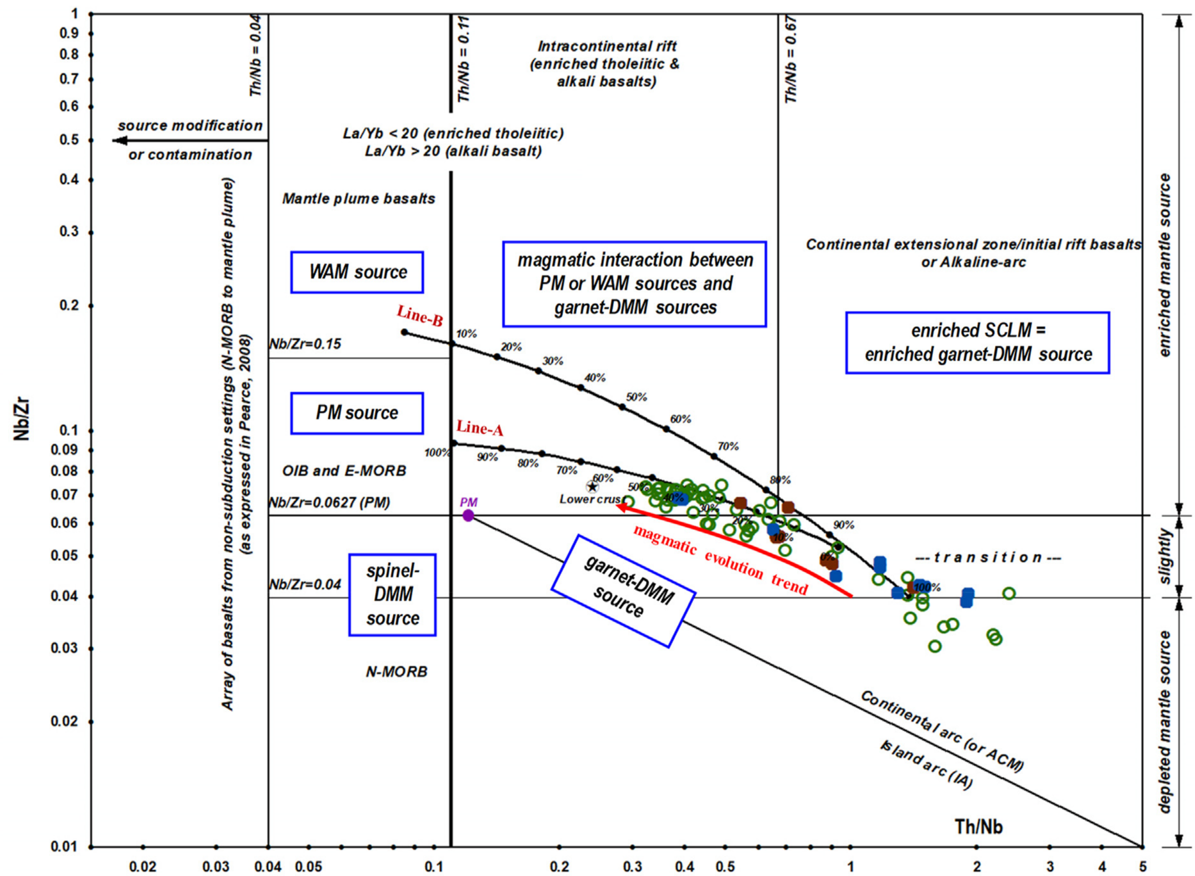

Fig. 7. The 3rd generation tectonic discrimination diagram of Nb/Zr vs. Th/Nb (developed after Saputro et al., 2022; Sun et al., 2006). The discrimination for enriched and depleted mantle sources using Nb/Zr is adapted from Le Roex et al. (1983). The -A and -B lines represent the mixing lines between the ocean island basalts/OIB or OIB-like (PM source) and mantle-plume (WAM source) with continental crust (garnet-DMM source), respectively (adopted from Wei et al., 2014). SCLM is a subcontinental lithospheric mantle. The Primitive Mantle (PM) source encompasses spinel and/or garnet PM, likewise with the Western Anatolian Mantle (WAM) source. PM and WAM originate from the asthenospheric mantle, whereas DMM is from the lithospheric mantle (see the analog diagram in Figs. 4 and 5). Symbols for Sumbing and Slamet Volcanics are shown in Fig. 2.

asthenosphere through the slab window beneath Central Java. However, it contradicts the previous opinions expressed by Vukadinovic and Nicholls (1989), who concluded that the Slamet volcanics are a product of IA. Similarly, Harijoko et al. (2020), who also stated that these volcanics are formed from IA settings based on observations of spidergram trends, referring to IA data from Sun (1980).

5.2. Geochemical comparison with Merapi and back-arc Muria volcanics

For comparison, the Merapi volcano, situated approximately 42 km (km) east of Sumbing volcano and 170 km east of Slamet volcano, exhibits lower Nb/La (<0.25) and low Nb/Y ratios (0.12–0.22) plotted only within the lithospheric mantle source (Abdel-Rahman, 2002, Fig. 6). Furthermore, Merapi volcanic rocks also display lower Nb/Zr ratios (0.0299–0.0412) (Gertisser and Keller, 2003), interpreted as being entirely the result of ACM tectonics (Fig. 8). Despite forming in the same ACM settings as Sumbing-Slamet, Merapi volcanics exhibit an opposite magmatic evolution trend (Figs. 6, 8 and 9) and have lower dTa values (0.22–0.40, as shown in Fig. 12), indicating a product solely of continental crust material and unmixed with other magma from asthenospheric sources (see combined Figs. 6, 8 and 9).

In another comparison, we specifically examine data for the Javanese back-arc volcano of Muria (Kirchenbaur et al., 2022), composed of a shoshonitic series (Fig. 2), mineralogically referred to as leucite-bearing absarokite, with higher Nb/Zr ratios (>0.15) and an increase in Rb values (182–437 ppm) relative to Zr (190–313 ppm) compared to the Sumbing-Slamet-Merapi volcanics, plotted within the post-collision fields (see the data depicted in Fig. 9). The tectonic formation of the back-arc Muria is suggested to be unrelated to subduction in Central Java and is interpreted to have formed from the exhumation of enriched mantle fragments originating from mantle-plume sources (see Muria plot results in Fig. 4). The tectonic setting of the back-arc Muria (northern Central Java) is more connected to the existence of the Tertiary Luk Ulo granitoid in Karangsambung (southern Central Java), which also formed from post-collision tectonics (Aminuddin et al., 2023), and it is suggested that they were produced in

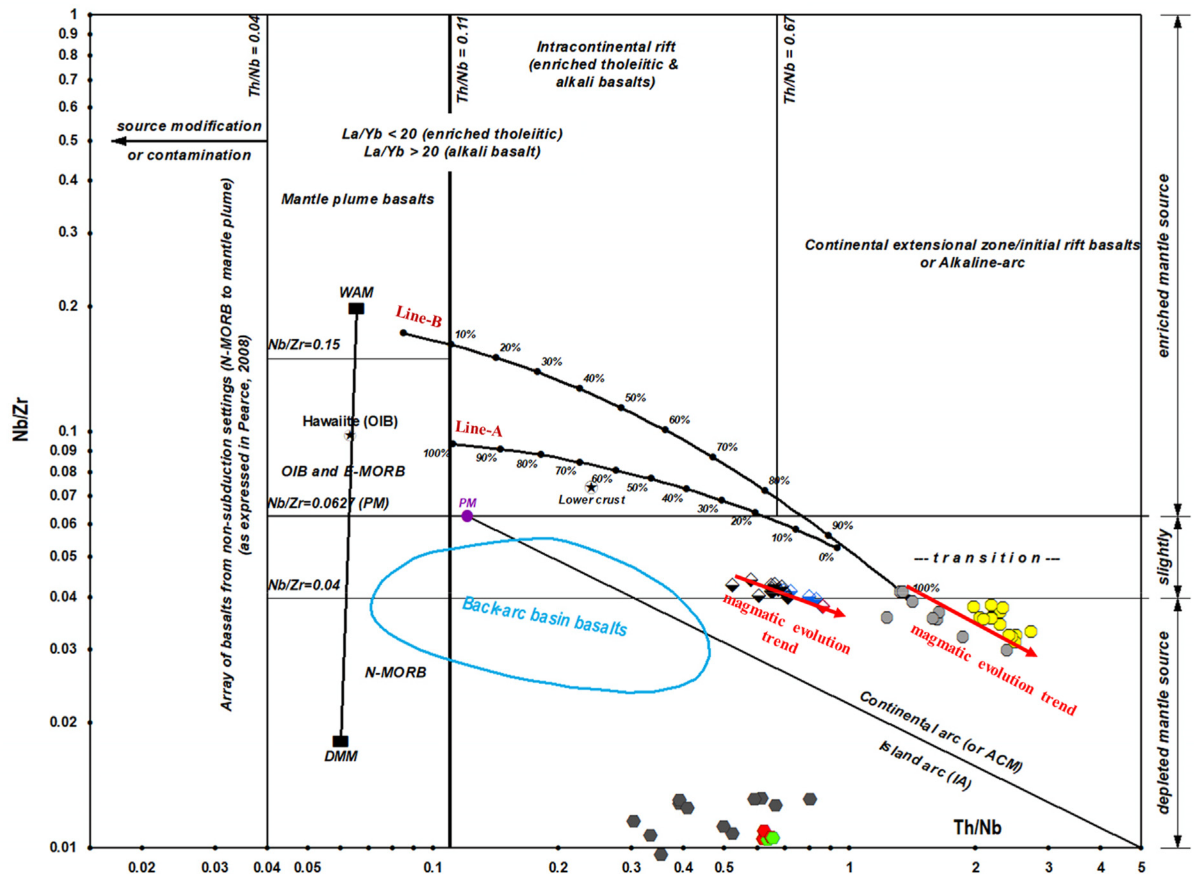

Fig. 8. The tectonic discrimination diagram of Nb/Zr vs. Th/Nb. Symbols for Merapi, Agung, and Candlemass-Vindication Volcanics are shown in Figs. 2 and 4. The WAM-DMM line represents a magmatic trend influenced by the oceanic environment, while the trend lines of -A and -B represent a magmatic evolution of WAM and PM mantle sources that are influenced by the continental environment. The boundary of back-arc basin basalts from Xia and Xu (2019).

the post-collisional period during the formation of the suture zone, which runs along from Ciletuh (West Java)–Luk Ulo (Karang Sambung, southern Central Java) and Muria (northern Central Java)–Meratus (South Borneo) (see Batara and Xu, 2022; Wang et al., 2023).

The isotopic trend of the back-arc Muria volcanic represents a continuation of mantle-plume magmatism evolution (see plot results of Wan-Su Basalts (Zhang et al., 2009) and Weizhou Island Basalt (Zhang et al., 2020) in Figs. 4 and 15), while the Sumbing-Slamet-Merapi trend is associated with arc magmatism.

5.3. Geochemical comparison with other arc-related volcanics

To ensure the objectivity and comparability of our research, we also collected and plotted data sets from other regions outside Java Island, such as the Agung volcanics in Bali Island, which still represent the same arc as the Sumbing-Slamet volcanics (Sunda-Banda arc; Dempsey, 2013), and the Candlemass-Vindication volcanics in the South Atlantic Ocean, representing a different arc (South Sandwich arc; Leat et al., 2003), for detailed comparison.

The plots in Fig. 6 reveal that the Agung volcanics exhibit a magmatism trend leading to the post-subduction field, interpreted as tending towards assimilation with post-orogenic magmatism (alkaline post-subduction) or deeper subducted alkaline magmatism. The magmatic evolution trend of the Agung volcanics differs from that of the Sumbing-Slamet volcanics, which point towards the upper right and interact with asthenospheric materials (Nb/La >0.6), caused by slab failure (indicated by Nb/Y > 0.4 in Fig. 5; Whalen and Hildebrand, 2019). The Agung volcanics are plotted separately from Sumbing-Slamet and fall within arc-transitional to continental arc fields (Fig. 6; after Cabanis and Lecolle, 1989). Most of the data have a Th/La ratio above 0.2 (precisely in the range 0.16–0.30), indicating involvement in oceanic slab melting and continental subducted sediment recycling. The tectonic formation is strongly suggested to have formed from ACM tectonics rather than an island arc (see Fig. 8).

In contrast to the Agung volcanics, the Candlemass-Vindication volcanics, as the most typical volcanics formed by IA tectonics, are characterized by low-K (tholeiitic series), low Nb/Zr (<0.0150), low La/Yb (<3), low Nb/La (<0.35), and low Nb/Y, resulting in plots falling within the IA field and significantly separated from the geochemical assemblage of Sumbing-Slamet, Merapi, and Agung volcanics (combined Figs. 2, 4, 6 and 8). Additionally, these IA volcanics have a low Th/La ratio (<0.2), strongly indicating that they are purely a product of oceanic crust (Wang et al., 2016). Typically,

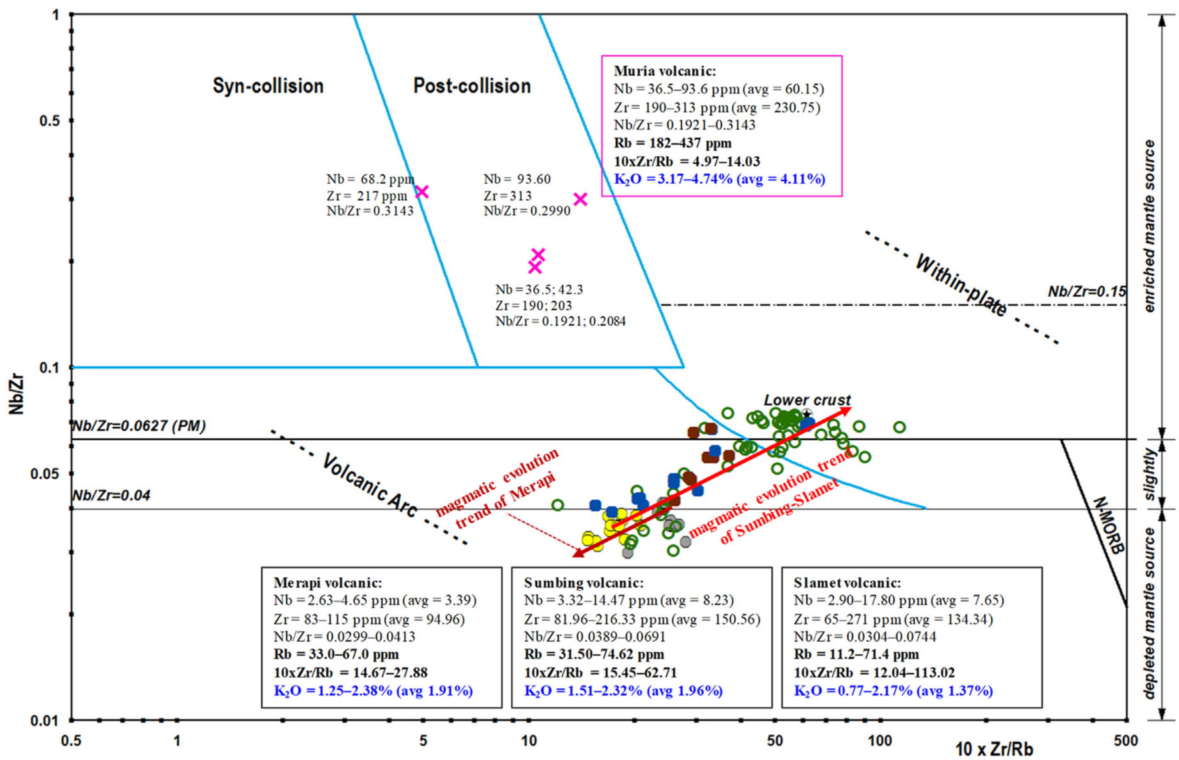

Fig. 9. The tectonic discrimination diagram of Nb/Zr vs. 10 × Zr/Rb (modified after ternary Harris et al., 1986). Symbols in Fig. 2.

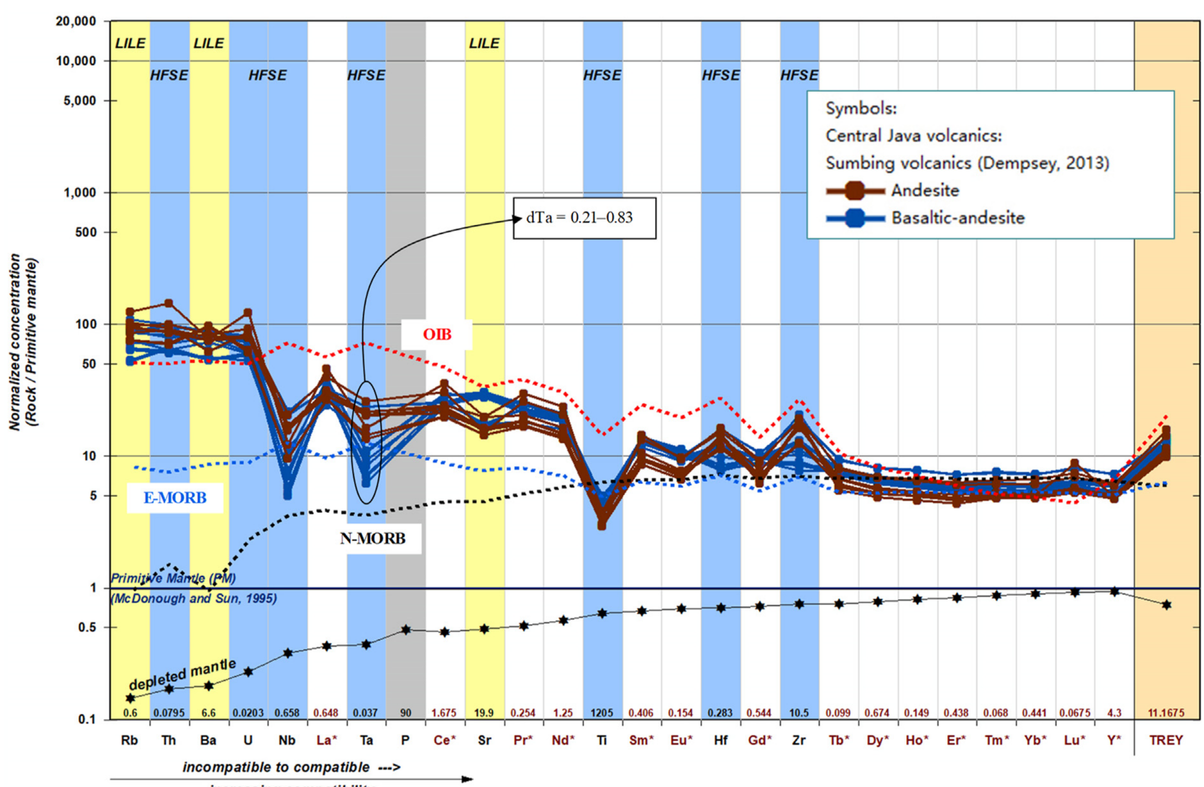

Fig. 10. The trace element abundance plot of Sumbing volcanics in order of increasing mantle compatibility (the incompatibility sequence is adopted from Zhang, 2014). The PM values are from McDonough and Sun (1995), depleted mantle (DM) from Salters and Stracke (2004). The dashed lines of N-MORB, E-MORB, and OIB from Sun and McDonough (1989).

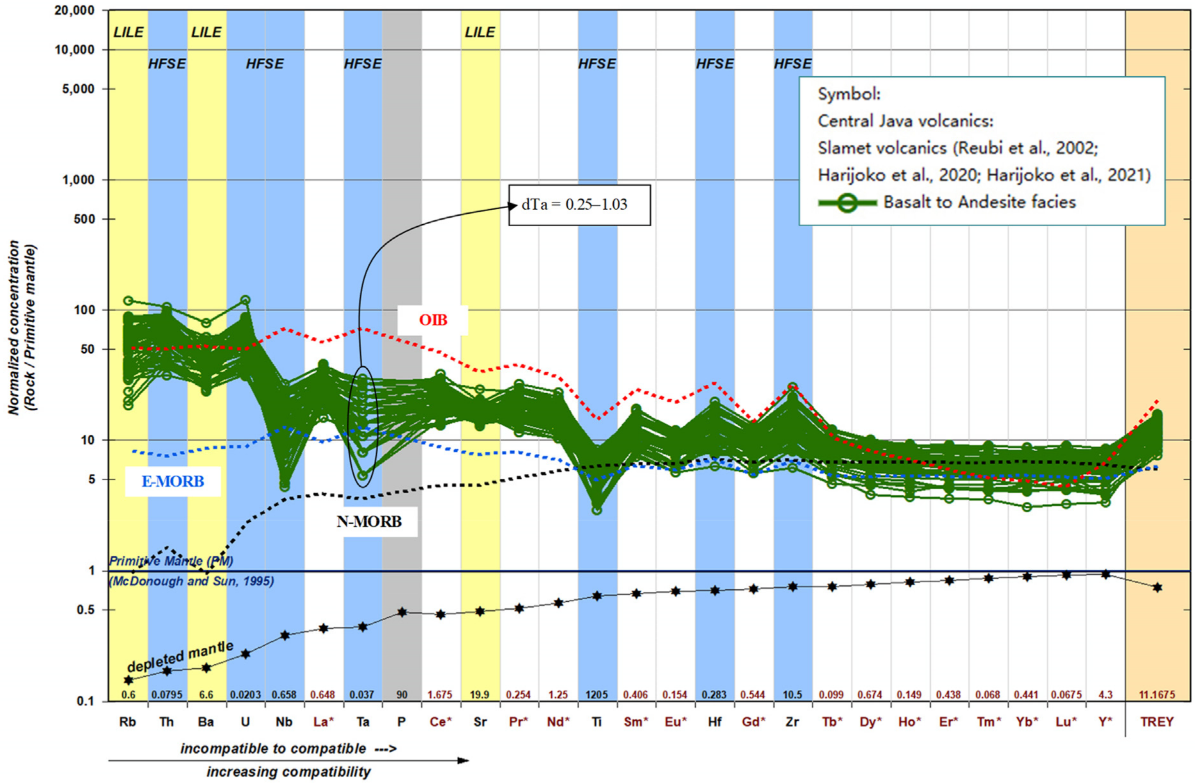

Fig. 11. The trace element abundance plot of Slamet volcanics.

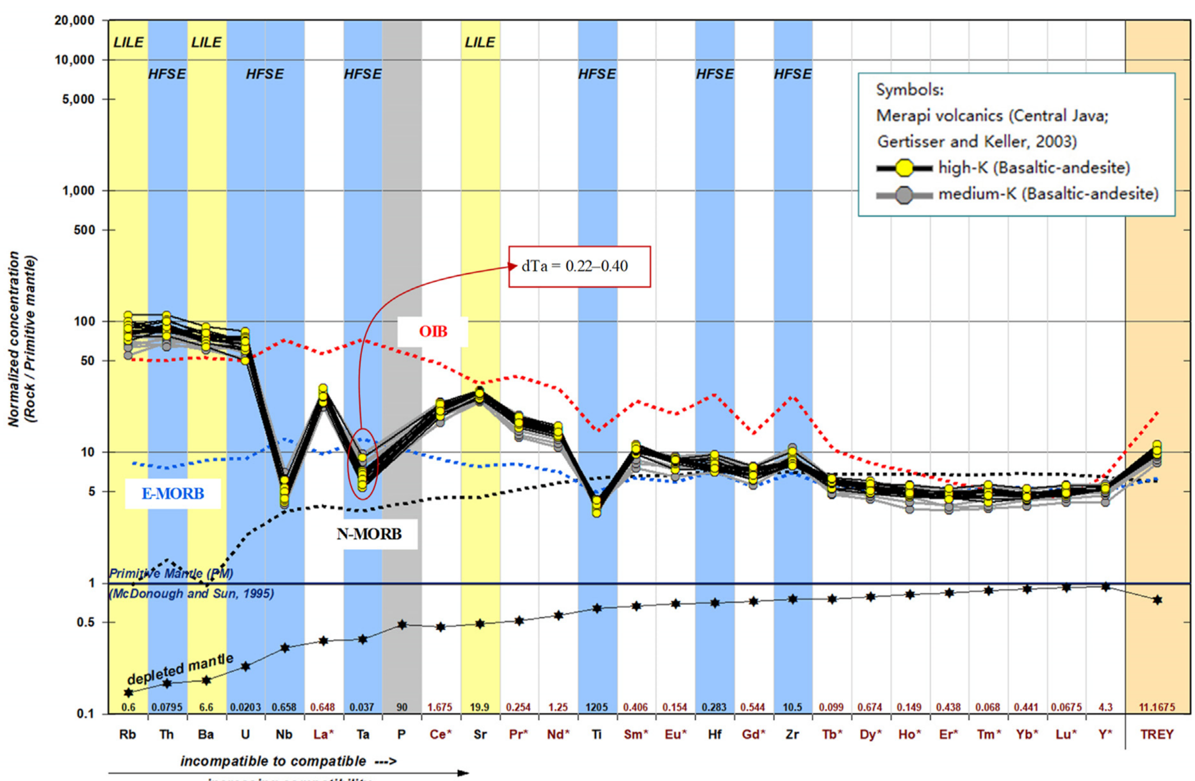

Fig. 12. The trace element abundance plot of Merapi volcanics.

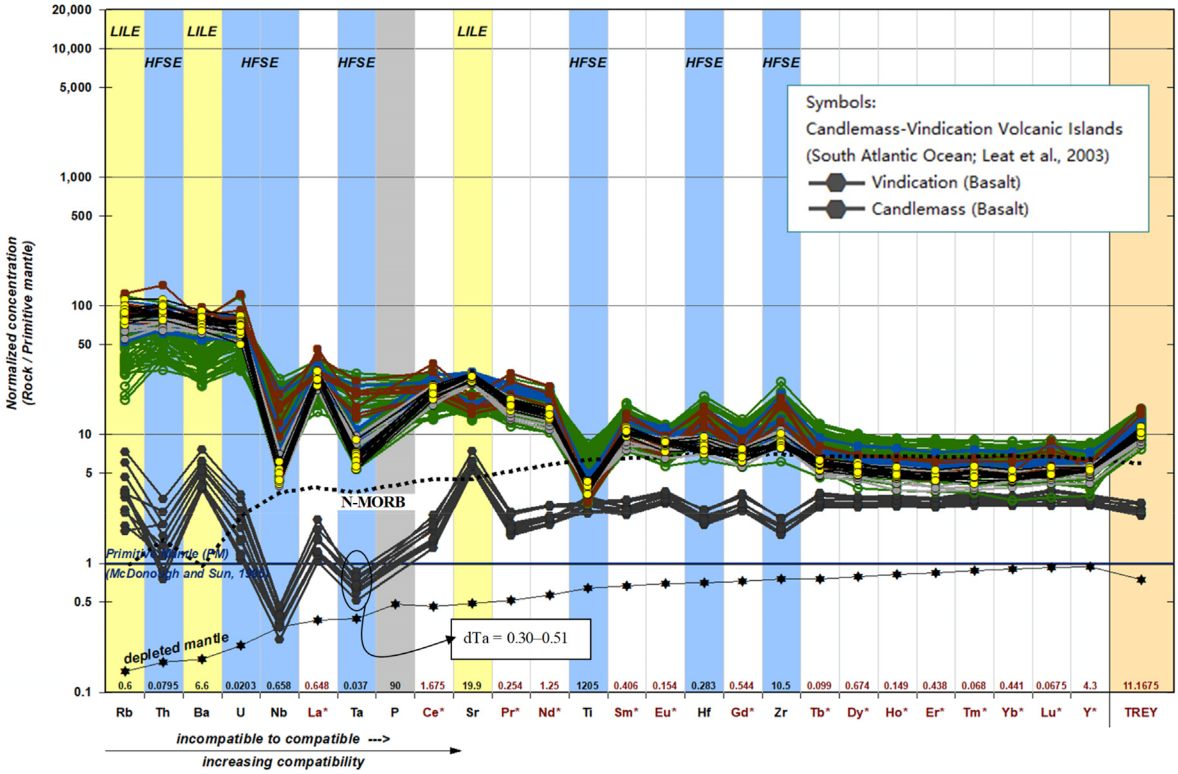

Fig. 13. The trace element abundance plots for Sumbing-Slamet-Merapi volcanics (Central Java) and Candlemass-Vindication volcanics (South Sandwich arc, South Atlantic Ocean; Leat et al., 2003).

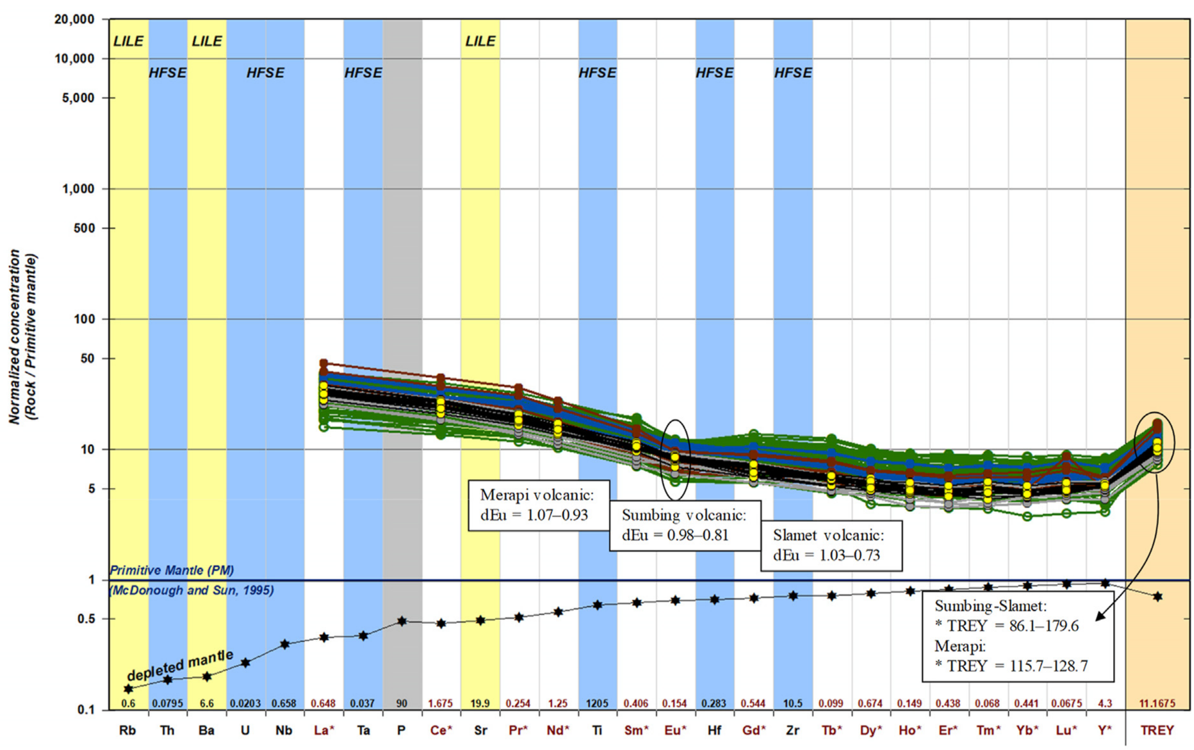

Fig. 14. The REEs abundance plots for Sumbing-Slamet-Merapi volcanics (Central Java).

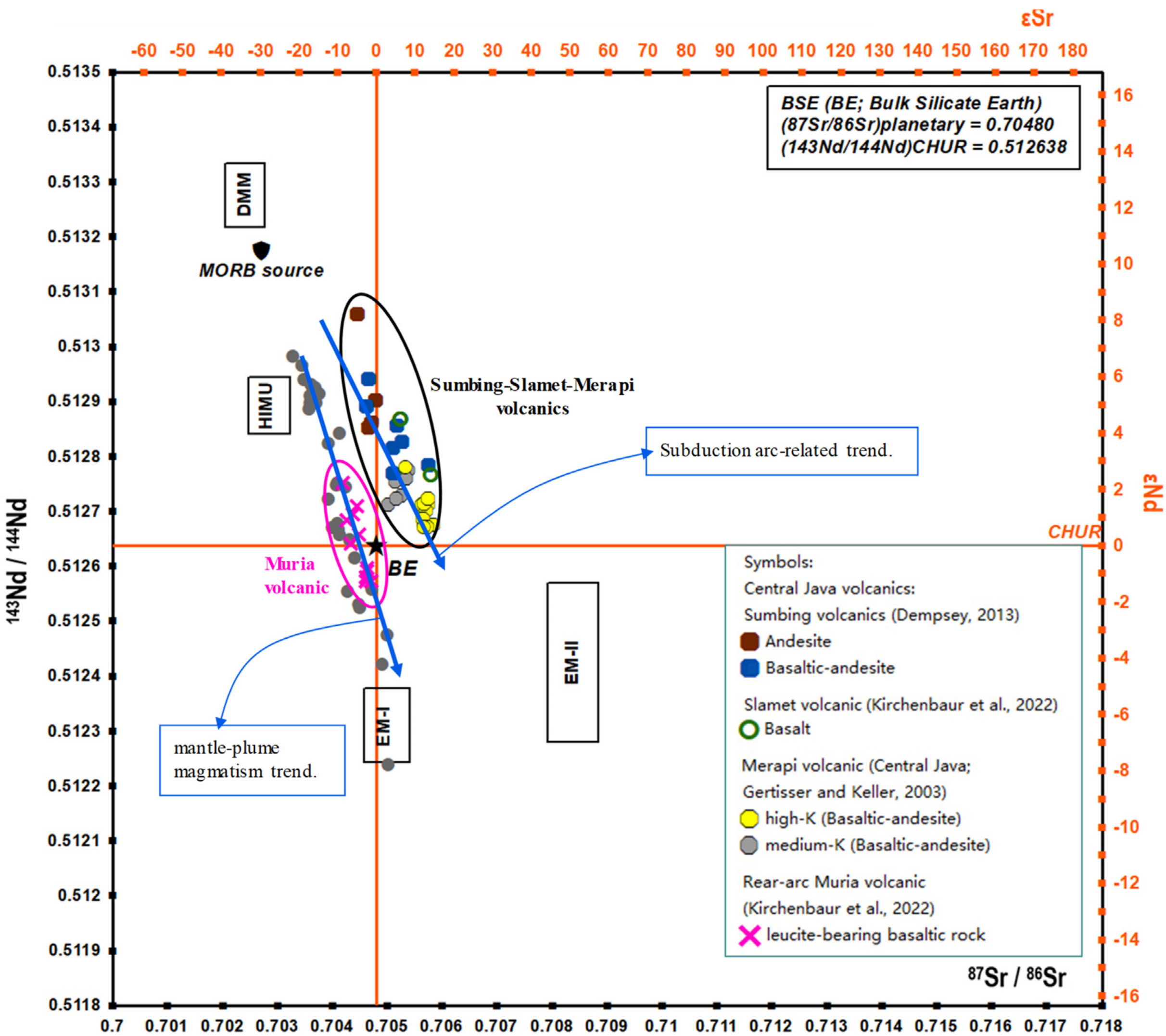

Fig. 15. The isotopic $^{143}Nd/^{144}Nd$ vs. $^{87}Sr/^{86}Sr$ diagram. The isotopic Nd–Sr of Slamet is taken from Kirchenbaur et al. (2022). The gray solid circle symbol is the dataset of mantle-plume from Wan-Su Basalts (Eastern China; Zhang et al., 2009) and Weizhou Island Basalt (Hainan, China; Zhang et al., 2020). Other symbols are in Fig. 4.

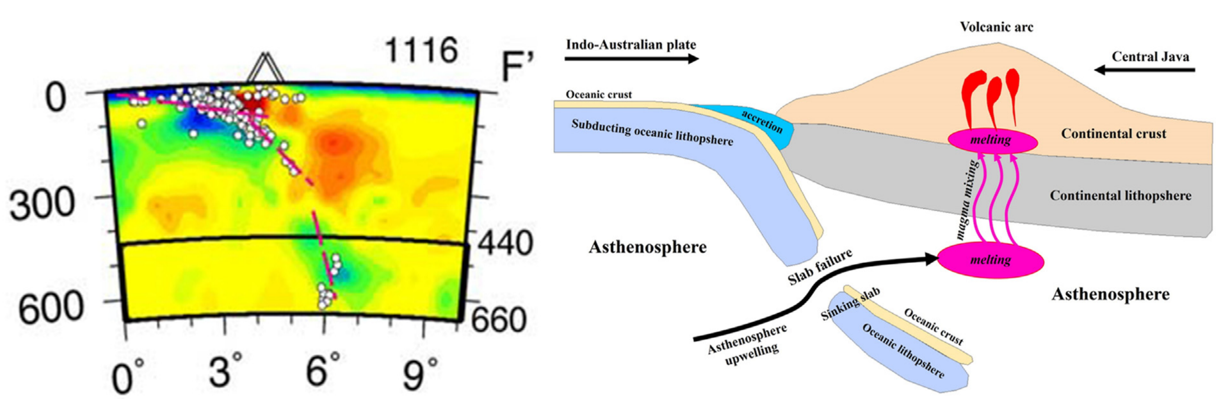

Fig. 16. Left: Slab tearing (failure) in the northern part of Central Java at a depth of about 300 km (Widiyantoro et al., 2011). Right: Cartoon illustration of the tectonic evolution model of Sumbing-Slamet's magmatism (Central Java) due to slab failure.

volcanic rocks from IAs exhibit characteristic depletion of high-field strength elements (HFSE, such as Nb–Ta and Zr–Hf) and Th–U relative to the more fluid-mobile large-ion lithophile elements (LILE, such as Rb and Ba) (Fig. 13). Magma resulting from typical IA tectonics is characterized by distinct negative spikes in Th, Nb, Ta, and negative Ta-anomaly (dTa = 0.30–0.51; Fig. 13). We also highlight here that the spidergram patterns of igneous rocks resulting from IAs differ from those from continental arcs, although both continental arcs and IAs exhibit the same negative Nb–Ta-anomaly trends.

6. Conclusions

In conclusion, our investigation into the geochemical characteristics and tectonic origins of the Sumbing-Slamet volcanics in Central Java provides valuable insights into the processes associated with slab failure in the region. Through comprehensive geochemical analysis and comparison with other volcanic formations, we have elucidated the complex magmatic evolution and tectonic settings of these volcanics. Our findings support the hypothesis of slab tearing beneath Central Java, as evidenced by the distinct geochemical signatures and magmatic interactions observed in the Sumbing-Slamet volcanics.

Based on geochemical data indicating medium to high-K, low TiO_2 relative to Al_2O_3 [$TiO_2 < (-1.1610 + 0.1935 \times Al_2O_3)$], relatively low Nb/Y < 0.6561 (sub-alkaline), a wide range of Nb/La (0.14–0.89), Nb/Zr in the range 0.0304–0.0744, Th/La >0.2, and low to high δTa (0.21–1.03), we conclude that the magmatism of Sumbing-Slamet volcanics is strongly indicative of formation within the tectonic context of the continental arc at the ACM, involving subducted sediment input. These magmatic processes are thought to be the result of mixing between lithospheric and asthenospheric mantle sources involving the magma from garnet-DMM and PM due to slab failure in Central Java, Indonesia.

Funding

This study was supported by the National Natural Science Foundation of China (No. 92162103), the Natural Science Foundation of Hunan Province (No. 2022JJ30699, No. 2023JJ10064), and the Science and Technology Innovation Program of Hunan Province (No. 2021RC4055, No. 2022RC1182).

Data availability

The raw data supporting the conclusions of this article will be made available by the author, with due reservation.

CRediT authorship contribution statement

Shaban Godang: Writing – review & editing, Writing – original draft, Visualization, Validation, Methodology, Investigation, Formal analysis, Conceptualization. **Sugeng Purwo Saputro:** Writing – review & editing, Writing – original draft, Visualization, Validation, Resources, Methodology, Investigation, Formal analysis, Conceptualization. **Huan Li:** Writing – review & editing, Validation, Supervision.

Declaration of competing interest

The authors declare that they have no known competing financial interests or personal relationships that could have appeared to influence the work reported in this paper.

Acknowledgments

The authors would like to express their gratitude to Dr. Daniel Müller of Santiago de Chile for his valuable input and contributions to improving the manuscript. We are also thankful to Dr. Scott Robert Dempsey for providing the geochemical data on the Sumbing volcanics in Central Java.

Appendix A. Supplementary data

Supplementary data to this article can be found online at https://doi.org/10.1016/j.sesci.2024.100199.

References

Abdel-Rahman, A.M., 2002. Mesozoic volcanism in the Middle East: geochemical, isotopic and petrogenic evolution of extension related alkali basalts from Central Lebanon. Geol. Mag. 139 (6), 621–640.

Aldanmaz, E., Köprübaşı, N., Gürer, Ö.F., Kaymakçı, N., Gourgaud, A., 2006. Geochemical constraints on the Cenozoic, OIB-type alkaline volcanic rocks of NW Turkey: implications for mantle sources and melting processes. Lithos 86 (1–2), 50–76.

Aminuddin, Muhammad Irman Khalif Bin Ahmad, Shuaib, Mohd, Akhtar, Naseem, Imam Setiawan, Nugroho, Warmada, I Wayan, 2023. U-Pb zircon geochronology and geochemistry of late cretaceous-paleocene metapsammite and metagranite of Luk Ulo Karangsambung, central Java, Indonesia. Research Square 1–38. https://doi.org/10.21203/rs.3.rs-2526917/v1.

Barrett, T.J., MacLean, W.H., 1997. Volcanic sequences, lithogeochemistry, and hydrothermal alteration in some bimodal volcanic-associated massive sulfide systems. Rev. Econ. Geol. 8, 101–132. https://doi.org/10.5382/Rev.08.05.

Batara, B., Xu, Changhai, 2022. Evolved magmatic arcs of South Borneo: insights into cretaceous slab subduction. Gondwana Res. 111, 142–164. https://doi.org/10.1016/j.gr.2022.08.001.

Cabanis, B., Lecolle, M., 1989. Le diagramme La/l0-Y/15-Nb/8: un outil pour la discrimination des séries volcaniques et la mise en évidence des processus de mélange et/ou de contamination crustale. Comptes Rendus de l'Academie des Sciences, Paris, series 2 (313), 2023–2029. ISSN 0764-4450.

Calanchi, N., Peccerillo, A., Tranne, C.A., Lucchini, F., Rossi, P.L., Kempton, P., Barbieri, M., Wu, T.W., 2002. Petrology and geochemistry of volcanic rocks from the island of Panarea: implications for mantle evolution beneath the Aeolian island arc (southern Tyrrhenian sea). J. Volcanol. Geoth. Res. 115 (3–4), 367–395. https://doi.org/10.1016/S0377-0273(01)00333-X.

Chotin, P., Rasplus, L., Rampnoux, J.P., Suminta, N.H., 1984. Major strike slip fault zone and associated sedimentation in the central part of Java island (Indonesia). Bull Soc Geol France 6, 1259–1268 (*in French*).

Coleman, R.G., Peterman, Z.E., 1975. Oceanic plagiogranite. J. Geophys. Res. 80 (8), 1099–1108. https://doi.org/10.1029/JB080i008p01099.

Cottam, M., Hall, R., Cross, L., Clements, B., Spakman, W., 2010. Neogene subduction beneath Java, Indonesia: slab tearing and changes in magmatism. Geophys. Res. Abstr. 12, 12437.

Dempsey, Scott Robert, 2013. Geochemistry of volcanic rocks from the Sunda arc. Durham University, p. 307. Doctoral thesis. http://etheses.dur.ac.uk/6948/.

Dong, Zhen, Tao, Chunhui, Liang, Jin, Liao, Shili, Li, Wei, Zhang, Guoyin, Cao, Zhimin, 2021. Geochemistry of basalts from southwest Indian ridge 64°E: implications for the mantle heterogeneity east of the melville transform. Minerals 11, 175. https://doi.org/10.3390/min11020175, 2021.

Fadlin, Fadlin, Godang, S., Ariyanti, N., Hamzah, W.N., Aditama, M.R., 2021. Tholeiitic basalt in banyumas basin (kebasen, central Java): the evidence of sedimentary recycling input and the contribution of oceanic slab on fore-arc active continental margin (ACM) magmatism. Indonesian Journal on Geoscience 8 (2), 233–253. https://doi.org/10.17014/ijog.8.2.233-253.

Foley, Stephen, Tiepolo, Massimo, Vannucci, Riccardo, 2002. Growth of early continental crust controlled by melting of amphibolite in subduction zones. Nature 417 (6891). https://doi.org/10.1038/nature00799.

Frisch, Wolfgang, Meschede, Martin, Blakey, Ronald, 2011. Plate Tectonics - Continental Drift and Mountain Building. Springer-Verlag Berlin Heidelberg, p. 217. https://doi.org/10.1007/978-3-540-76504-2.

Gardner, M.F., Troll, V.R., Gamble, J.A., Gertisser, R., Hart, G.L., Ellam, R.M., Harris, C., Wolff, J.A., 2013. Crustal differentiation processes at Krakatau volcano, Indonesia. J. Petrol. 54 (1), 149–182. https://doi.org/10.1093/petrology/egs066.

Gertisser, R., Keller, J., 2003. Trace element and Sr, Nd, Pb, and O isotope variations in medium-K and high-K volcanic rocks from Merapi volcano, central Java, Indonesia: evidence for the involvement of subducted sediments in Sunda arc magma genesis. J. Petrol. 44 (3), 457–489. https://doi.org/10.1093/petrology/44.3.457.

Hall, R., Spakman, W., 2015. Mantle structure and tectonic history of SE Asia. Tectonophysics 658, 14–45.

Hamilton, W., 1979. Tectonics of the Indonesian Region, vol. 1078. U.S. Geological Survey Professional Paper, p. 345.

Handley, H.K., Davidson, Jon P., Macpherson, Colin G., Stimac, James A., 2008. Untangling differentiation in arc lavas: constraints from unusual minor and trace element variations at Salak Volcano, Indonesia. Chem. Geol. 255, 360–376. https://doi.org/10.1016/j.chemgeo.2008.07.007.

Handley, H.K., Blichert-Toft, J., Gertisser, R., Macpherson, C.G., Turner, S.P., Zaennudin, A., Abdurrachman, M., 2014. Insights from Pb and O isotopes into along-arc variations in subduction inputs and crustal assimilation for volcanic rocks in Java, Sunda arc Indonesia. Geochem. Cosmochim. Acta 139, 205–226.

Harijoko, Agung, Uruma, Ryusuke, Wibowo, Haryo Edi, Setijadji, Lucas Doni, Imai, Akira, Yonezu, Kotaro, KoichiroWatanabe, 2016. Geochronology and magmatic evolution of the Dieng Volcanic Complex, Central Java, Indonesia and their relationships to geothermal resources. J. Volcanol. Geoth. Res. 310, 209–224. https://doi.org/10.1016/j.jvolgeores.2015.12.010.

Harijoko, Agung, N Milla, A., E Wibowo, H., Setiawan, N.I., 2020. Magma evolution of Slamet volcano, central Java, Indonesia based on lava characteristic. IOP Conf. Ser. Earth Environ. Sci. 451, 012092. https://doi.org/10.1088/1755-1315/451/1/012092.

Harijoko, Agung, Sari, Sistien Adhaena, Wibowo, Haryo Edi, Setiawan, Nugroho Imam, Moktikanana, Mradipta Lintang Alifcanta, 2021. Stratigraphy, chronology, and magma evolution of Holocene volcanic products from Mt. Slamet deposited in the Guci Valley, Central Java, Indonesia. J. Volcanol. Geoth. Res. 418, 107341. https://doi.org/10.1016/j.jvolgeores.2021.107341.

Harris, N.B.W., Pearce, J.A., Tindle, A.G., 1986. Geochemical characteristics ofcollision-zone magmatism. In: Coward, M.P., Ries, A.C. (Eds.), Collision Tectonics, Geological Society, vol. 19. Special Publication, London, pp. 67–81.

Hatherton, Trevor, Dickinson, William R., 1969. The relationship between andesitic volcanism and seismicity in Indonesia, the lesser antilles, and other island arcs. J. Geophys. Res. 74 (22). https://doi.org/10.1029/jb074i022p05301.

Hawkesworth, C.J., Turner, S.P., McDermott, F., Peate, D.W., van Calsteren, P., 1997. U-Th isotopes in arc magmas: implications for element transfer from the subducted crust. Science 276 (5312), 551–555.

Hoffmann-Rothe, A., Ritter, O., Haak, V., 2001. Magnetotelluric and geomagnetic modelling reveals zones of very high electrical conductivity in the upper crust of Central Java. Phys. Earth Planet. In. 124 (3–4), 131–151.

Katili, J.A., 1978. Past and present geotectonic position of Sulawesi, Indonesia. Tectonophysics 45, 289–322.

Kirchenbaur, M., Schuth, S., Barth, A.R., Luguet, A., König, S., Idrus, A., Garbe-Schönberg, D., Münker, C., 2022. Sub-arc mantle enrichment in the Sunda rear-arc inferred from HFSE systematics in high-K lavas from Java. Contrib. Mineral. Petrol. 177, 8. https://doi.org/10.1007/s00410-021-01871-9.

Koulakov, I., Bohm, M., Asch, G., Lühr, B.G., Manzanares, A., Brotopuspito, K.S., Fauzi, P., Purbawinata, M.A., Puspito, N.T., Ratdomopurbo, A., Kopp, H., Rabbel, W., Shevkunova, E., 2007. P and S velocity structure of the crust and the upper mantle beneath central Java from local tomography inversion. J. Geophys. Res. Solid Earth 112, 1–19.

Kundu, B., Gahalaut, V.K., 2011. Slab detachment of subducted Indo-Australian plate beneath Sunda arc, Indonesia. J. Earth Syst. Sci. 120 (2), 193–204. https://doi.org/10.1007/s12040-011-0056-7.

Leat, P.T., Smellie, J.L., Millar, I.L., Larter, R.D., 2003. Magmatism in the South Sandwich Arc, vol. 219. Geological Society, London, Special Publications, pp. 285–313. https://doi.org/10.1144/GSL.SP.2003.219.01.14.

Lee, C.-T.A., Shen, B., Slotnick, B.S., Liao, K., Dickens, G.R., Yokoyama, Y., Lenardic, A., Dasgupta, R., Jellinek, M., Lackey, J.S., Schneider, T., Tice, M.M., 2012. Continental arc-island arc fluctuations, growth of crustal carbonates, and long-term climate change. Geosphere 9 (1). https://doi.org/10.1130/ges00822.1.

Le Roex, A.P., Dick, H.J.B., Erlank, A.X., Reid, A.M., Frey, F.A., Hart, S.R., 1983. Geochemistry, mineralogy and petrogenesis of lavas erupted along the southwest Indian ridge between the bouvet triple junction and 11 degrees east. J. Petrol. 24 (3), 267–318.

Leterrier, J., Yuwono, Y.S., Soeria-Atmadja, R., Maury, R.C., 1990. Potassic volcanism in central Java and South sulawesi, Indonesia. J. Asian Earth Sci. 4 (3), 171–187. https://doi.org/10.1016/s0743-9547(05)80011-x.

McDonough, W.F., Sun, S.S., 1995. The composition of the Earth. Chem. Geol. 120 (3–4), 223–253.

Müller, D., Groves, D.I., 1993. Direct and indirect associations between potassic igneous rocks, shoshonites and gold-copper deposits. Ore Geol. Rev. 8 (5), 383–406.

Mulyaningsih, Sri., Shaban, Godang, 2020. Geochemistry of basaltic merbabu volcanic rocks, central Java, Indonesia. Indonesian Journal on Geoscience 7 (2), 161–178. https://doi.org/10.17014/ijog.7.2.161-178.

Peccerillo, A., Taylor, S.R., 1976. Geochemistry of Eocene calc-alkaline volcanic rocks from the Kastamonu area, northern Turkey. Contrib. Mineral. Petrol. 58, 63–81. https://doi.org/10.1007/BF00384745.

Pearce, J.A., 1996. A user's guide to basalt discrimination diagrams. In: Bailes, A.H., Christiansen, E.H., Galley, A.G., Jenner, G.A., Keith, Jeffrey D., Kerrich, R., Lentz, D.R., Lesher, C.M., Lucas, S.B., Ludden, J.N., Pearce, J.A., Peloquin, S.A., Stern, R.A., Stone, W.E., Syme, E.C., Swinden, H.S., Wyman, D.A. (Eds.), Trace Element Geochemistry of Volcanic Rocks, Applications for Massive Sulphide Exploration, Short Course Notes, vol. 12. Geological Association of Canada, pp. 79–113.

Pettke, Thomas, Kodolányi, János, Kamber, Balz S., 2018. From ocean to mantle: new evidence for U-cycling with implications for the HIMU source and the secular Pb isotope evolution of Earth's mantle. Lithos 316–317, 66–76. https://doi.org/10.1016/j.lithos.2018.07.010.

Puspito, N.T., Yamanaka, Y., Miyatake, T., Shimazaki, K., Hirahara, K., 1993. Three-dimensional P-wave velocity structure beneath the Indonesian region. Tectonophysics 220, 175–192.

Reubi, O., Nicholls, I.A., Kamenetsky, V.S., 2002. Early mixing and mingling in the evolution of basaltic magmas: evidence from phenocryst assemblages, Slamet Volcano, Java, Indonesia. J. Volcanol. Geoth. Res. 119, 255–274. https://doi.org/10.1016/s0377-0273(02)00357-8.

Salters, V.J.M., Stracke, A., 2004. Composition of the depleted mantle. G-cubed 5 (5), Q05B07.

Saputro, S.P., Godang, S., Priadi, B., Basuki, N.I., Himawan, B., 2022. Geochemical study of Al-Fe-Ti enrichment in rock weathering: implications for the recognizing of igneous protolith and the enrichment of REE in soil profile. Appl. Geochem. 140 (2022), 105259.

Schaen, Allen J., Brian, R. Jicha, Suzanne, M. Kay, Brad, S. Singer, Ashley, Tibbetts, 2016. Eocene to pleistocene magmatic evolution of the delarof islands, aleutian arc. G-cubed 17 (3), 1086–1108. https://doi.org/10.1002/2015gc006067.

Shaban, G., Fadlin, F., Priadi, B., 2016. Geochemical signatures of potassic to sodic adang volcanics, western sulawesi: implications for their tectonic setting and origin. Indonesian Journal on Geoscience 3, 195–214.

Smyth, H., Hall, R., Hamilton, J.P., Kinny, P., 2005. East Java: cenozoic basins, volcanoes and ancient basement: Jakarta. Proceedings, Indonesian Petroleum Association Annual Convention 251–266, 30th.

Smyth, H.R., Hamilton, P.J., Hall, R., Kinny, P.D., 2007. The deep crust beneath island arcs: inherited zircons reveal a gondwana continental fragment beneath East Java, Indonesia. Earth Planet Sci. Lett. 258, 269–282.

Sugimura, A., 1968. In: Basalts, Hess, H.H., Poldervaart, A. (Eds.), Spatial Relations of Basaltic Magmas in Island Arcs, vol. 2. Interscience, pp. 537–571.

Sun, S.-S., 1980. Lead isotopic study of young volcanic rocks from mid-oceanic ridges, oceanic island and island arcs. Phil. Trans. Roy. Soc. Lond. 297, 409–445.

Sun, S.-S., McDonough, W.F., 1989. Chemical and isotopic systematics of oceanic basalts: implications for mantle composition and processes. In: Saunders, A.D., Norry, M.J. (Eds.), Magmatism in the Ocean Basins, vol. 42. Geological Society, London, Special Publications, pp. 313–345.

Sun, S.Q., Zhang, C.J., Huang, R.Q., 2006. The tectonic settings discrimination of the basalts in the convergent margin of plate by Th, Nb, and Zr. Adv. Earth Sci. 21 (6), 593–598 (*in Chinese*).

Vukadinovic, D., Nicholls, I.A., 1989. The petrogenesis of island arc hasalts from Gunung Slamet volcano, Indonesia: trace element and $^{87}Sr/^{86}Sr$ contraints. Geochem. Cosmochim. Acta 53 (9), 2349–2363. https://doi.org/10.1016/0016-7037(89)90357-8.

Vukadinovic, D., Sutawidjajat, Igan, 1995. Geology, mineralogy and magma evolution of gunung Slamet volcano, Java, Indonesia. J. Asian Earth Sci. 11 (2), 135–164. https://doi.org/10.1016/0743-9547(94)00043-e.

Wang, Chong, Peng, Peng, Wang, Xin-ping, Yang, Shu-yan, 2016. Nature of three Proterozoic (1680 Ma, 1230 Ma and 775 Ma) mafic dyke swarms in North China: implications for tectonic evolution and paleogeographic reconstruction. Precambrian Res. 285, 109–126.

Wang, D., Lin, F.C., Shi, M.F., Wang, H., Yang, X.Y., 2023. Geological setting, tectonic evolution and spatio-temporal distributions of main mineral resources in South East Asia: a comprehensive review. Solid Earth Sciences 8 (1), 34–48.

Whalen, Joseph B., Hildebrand, Robert S., 2019. Trace element discrimination of arc, slab failure, and A-type granitic rocks. Lithos 348–349, 105179. https://doi.org/10.1016/j.lithos.2019.105179.

Whitford, D.J., Nicholls, I.A., Taylor, S.R., 1979. Spatial variations in the geochemistry of quaternary lavas across the Sunda arc in Java and Bali. Contrib. Mineral. Petrol. 70 (3), 341–356. https://doi.org/10.1007/bf00375361.

Widiyantoro, S., van Der Hilst, R.D., 1996. Structure and evolution of lithospheric slab beneath the Sunda Arc, Indonesia. Science 271, 1566–1570. https://doi.org/10.1126/science.271.5255.1566.

Widiyantoro, S., van Der Hilst, R.D., 1997. Mantle structure beneath Indonesia inferred from high-resolution tomographic imaging. Geophys. J. Int. 130, 167–182. https://doi.org/10.1111/j.1365-246x.1997.tb00996.x.

Widiyantoro, S., Pesicek, J.D., Thurber, C.H., 2011. Subducting Slab Structure below the Eastern Sunda Arc Inferred from Non-linear Seismic Tomographic Imaging, vol. 355. Geological Society, London, Special Publications, pp. 139–155. https://doi.org/10.1144/sp355.7.

Wei, X., Xu, Y.-G., Feng, Y.-X., Zhao, J.-X., 2014. Plume-lithosphere interaction in the generation of the Tarim large igneous province, NW China: geochronological and geochemical constraints. Am. J. Sci. 314 (1), 314–356.

Xia, Yan, Xu, Xi-sheng, 2019. A fragment of columbia supercontinent: insight for cathaysia block basement from tectono-magmatic evolution and mantle heterogeneity. Geophys. Res. Lett. 46, 2012–2024.

Yu, Yang, Huang, Xiao-Long, Chung, Sun-Lin, Jie, Li, Lai, Yu-Ming, Setiawan, Iwan, Sun, Min, 2022. Molybdenum isotopic constraint from Java on slab inputs to subduction zone magmatism. Geochem. Cosmochim. Acta 332, 1–18. https://doi.org/10.1016/j.gca.2022.06.009.

Zhang, Jun-Jun, Zheng, Yong-Fei, Zi-Fu, Zhao, 2009. Geochemical evidence for interaction between oceanic crust and lithospheric mantle in the origin of Cenozoic continental basalts in east-central China. Lithos 110 (1–4), 305–326. https://doi.org/10.1016/j.lithos.2009.01.006.

Zhang, Y., Yu, K., Fan, T., Yue, Y., Wang, R., Jiang, W., Xu, S., Wang, Y., 2020. Geochemistry and petrogenesis of quaternary basalts from Weizhou island, northwestern South China sea: evidence for the hainan plume. Lithos 362–363 (June 2020), 105493. https://doi.org/10.1016/j.lithos.2020.105493.

Zhang, Youxue, 2014. Quantification of the elemental incompatibility sequence, and composition of the "superchondritic" mantle. Chem. Geol. 369, 12–21. https://doi.org/10.1016/j.chemgeo.2014.01.012.